A Nonredundant SVD-based Precoding Matrix for Blind Channel Estimation in CP-OFDM Systems Over Channels with Memory

Osamah J. Al-Qadhi[1*] and Laith A. Abdul-Rahaim[2]

[1*]Medical Instrumentation Techniques Engineering Department, Al-Mustaqbal University, Hillah, Iraq.
Department of Electrical Engineering, College Engineering, University of Babylon, Hillah, Iraq.
eng.usama2010@gmail.com, https://orcid.org/0000-0001-5893-1658

[2]Department of Electrical Engineering, College Engineering, University of Babylon, Hillah, Iraq.
drlaithanzy@uobabylon.edu.iq, https://orcid.org/0000-0001-8064-4401

Received: November 21, 2023; Accepted: January 10, 2024; Published: February 29, 2024

Abstract

In this paper, we investigate blind channel estimation in cyclic, prefixed orthogonal frequency division multiplexing (OFDM) systems using precoding matrices. Many studies show how the performance of bit error rate (BER) and mean square error of channel estimation are impacted by using a circulant matrix as a precoding matrix. We investigate a new structure for the precoding matrix in which the first row is generated by an exponentially decreasing equation along with the Toeplitz function and deploying singular value decomposition (SVD) to generate the final precoder matrix. This type of SVD-based precoding matrix has been presented and simulated under various circumstances. The resulting precoding matrix is employed in two different OFDM systems to estimate the channel frequency response vector up to scalar ambiguity. The proof of the precoding matrix full rank property is presented, along with other criteria that help with the development of various precoding matrices.

Keywords: OFDM, Blind Channel Estimation, Precoding, SVD, NMSE.

1 Introduction

One of the most effective spatially for broadband wireless communication is OFDM, which has drawn a lot of interest. Large manufacturers and standards are employing OFDM for a variety of applications, in addition to IEEE 802.11a wireless LAN, WiMAX for universal microwave access, LTE and LTE-Advanced, and digital video broadcasting (DVB), including terrestrial (DVB-T) and handheld (DVB-H) (Mostofi & Cox, 2005). It is extensively utilized in the current 4G and 5G technologies because of its high spectrum utilization and robust noise tolerance The unpredictable nature of the channel environment, combined with temporal oscillations, will seriously impair the quality of communication transmission during the signal transmission process (Al-Jzari & Iviva, 2015). After

Journal of Internet Services and Information Security (JISIS), volume: 14, number: 1 (February), pp. 282-305.
DOI: *10.58346/JISIS.2024.I1.018*

*Corresponding author: Medical Instrumentation Techniques Engineering Department, Al-Mustaqbal University, Hillah, Iraq; Department of Electrical Engineering, College Engineering, University of Babylon, Hillah, Iraq.

digitally modulating the transmitter's messages, the symbols are converted from frequency domain signals to time domain signals using an inverse fast Fourier transform (IFFT).

One of the main properties that makes OFDM attractive is its effectiveness in countering the spread of multipath delay. After IFFT, a guard interval is added between blocks of OFDM baseband signals to avoid inter-symbol interferences (ISI). So that multipath components of one symbol cannot interact with the following symbol, it is chosen to be bigger than the expected delay spread (Andersen, Rappaport, & Yoshida, 1995). In OFDM systems, there are two primary guard intervals: zero padding and cyclic prefix. While zeros are filled at the end of each symbol in a zero padding OFDM system, a copy of the final section of the same symbol is added to the symbol in a cyclic prefixed OFDM system.

For accurate demodulation of the transmitted signal, alignment, decoding, and many other baseband processing applications, it is very important to provide perfect and up-to-date channel knowledge. Therefore, channel estimation remains an important block at the stages of signal processing in the receiver of both present and developing wireless communication systems. Pilot-based estimation concepts, sometimes referred to as learning-based concepts, and blind channel estimation concepts are the two core ideas in channel estimation methods.

When a channel is estimated based on a pilot signal, the prior known pilot signals to the receiver are multiplexed with the data stream for channel estimation. These signals are configured in the usual ways, like comb-style or block-style. (Coleri, Ergen, Puri, & Bahai, 2002). A variety of training-based channel predictions are proposed in (Sari, Karam, & Jeanclaude, 1995) and (Li, Cimini, & Sollenberger, 1998). Unfortunately, applying training sequences decreases the system's effectiveness. Moreover, due to the fact that the channel in certain wireless applications experiences changes over time, it becomes necessary to transmit the training sequence at regular intervals, resulting in a further reduction in channel throughput. Blind channel estimation is accomplished by analyzing channel statistical information as well as the received signals. The advantage of a blind channel estimate is that there is no loss in bandwidth or throughput, but due to the amount of data needed, it can only be applied to channels that vary gradually over time (Heinz et al., 2021).

Blind channel estimation is available in a variety of ways, including statistical and deterministic approaches. Although the deterministic technique uses both channel coefficients and received signals as deterministic entities, the statistical channel estimation method does not benefit from the statistical properties of the received signals (Petropulu, Zhang, & Lin, 2004). One popular method for blindly estimating channels in OFDM systems is the subspace approach (Fan, Gao, & Xue, 2009; Fang, Chen, Lin, Shieh, & Hsu, 2015; Huang Xuejun, Bi Houjie, & Yu Songyu, 2003; Muquet, de Courville, & Duhamel, 2002; Yue & Zhou, 2011; Zeng & Ng, 2004), which relies on building overdetermined systems. Even at high signal-to-noise ratios, there are certain limitations with subspace blind estimation techniques, as demonstrated by a comparison of subspace methods in OFDM systems in (Al-Qadhi, Abdul-Rahaim, Sahib, Obaid, & Alwan, 2024). Recursive least squares (RLS) and least mean squares (LMS) algorithms are created using the subspace method in (Doukopoulos & Moustakides, 2004, 2006) to construct adaptive blind channel identification algorithms in zero-padded OFDM systems.

Another method for blindly estimating a channel is to use precoding techniques, which include adding a precoding block to the system at the transmitter. In (Petropulu & Ruifeng Zhang, 2002; Ruifeng Zhang, n.d.), a straightforward linear precoder that doesn't alter block length or give the system redundancy was proposed. The accuracy of the algorithm is greatly restricted due to its sole extraction of the channel from a single column of the covariance matrix, in contrast to the redundancy-introducing precoder. (Yongming, Hanwen, Yadong, & Jianguo, 2007), which estimates the frequency of the selective fading channel using auto-correlation and SVD operations. Conversely, the joint precoding technique estimation approach in (Gao & Nallanathan, 2007) utilizes the integer columns of the precoding matrix. First introduced in (Al-Qadhi, Semenov, Talib, Al-Barrak, & Al-Ghazali, 2024; Al-Qadhi, Semenov, Talib, Almufti, & Al-Ghazali, 2023), an SVD-based precoder employing an exponentially decaying function is used to create new models for channel estimation in OFDM systems at various guard intervals.

In this work, we study blind channel estimation using a symmetric precoding matrix based on SVD in a conventional OFDM system with a cyclic prefix. To compare the results of NMSE, we simulate another SVD-based precoding matrix proposed in (Al-Qadhi, Semenov, et al., 2024; Al-Qadhi et al., 2023) using two different OFDM system models. In the first model, each received OFDM symbol has a single precoding matrix, and the autocorrelation matrix of the received symbols is used for channel estimation, while the second model uses a block of four precoding matrices in order to precode two adjacent symbols and uses a cross correlation between the related received symbols. All SVD-based precoders are compared with the circulant precoder mentioned in (Lin & Petropulu, 2005), and the results of NMSE and BER are presented under various parameters of the OFDM symbol and SNR.

2 OFDM Channel Estimation with a Single Precoding Matrix

1) System Model

Figure 1 shows the linearly precoded OFDM system. Initially, the data stream is divided into several OFDM blocks. The information carrying symbols of the i-th block are denoted by $d_{i,m}, m = 0,1,\dots, N-1$ and N represents the length of the OFDM symbol. Let $d_{i,m}$. be zero-mean i.i.d., spatially uncorrelated, and temporally white unit variance. The following is a definition of the precoded symbols:

$$\boldsymbol{s}_{\boldsymbol{i}}^{(k)} = \boldsymbol{A}^{(k)}\boldsymbol{d}_{\boldsymbol{i}} \tag{1}$$

Where $\boldsymbol{d}_{\boldsymbol{i}} = [d_{i,0},\dots, d_{i,N-1}]^T$ is the data block and $\boldsymbol{s}_{\boldsymbol{i}}^{(k)} = [s_{i,0}^{(k)},\dots, s_{i,N-1}^{(k)}]^T$, k = 1 ,2 and 3 are the data vectors after the precoder, respectively $\boldsymbol{A}^{(1)}$, $\boldsymbol{A}^{(2)}$ and $\boldsymbol{A}^{(3)}$. There is no redundancy introduced into the systems because all precoding matrices are of size $N \times N$.

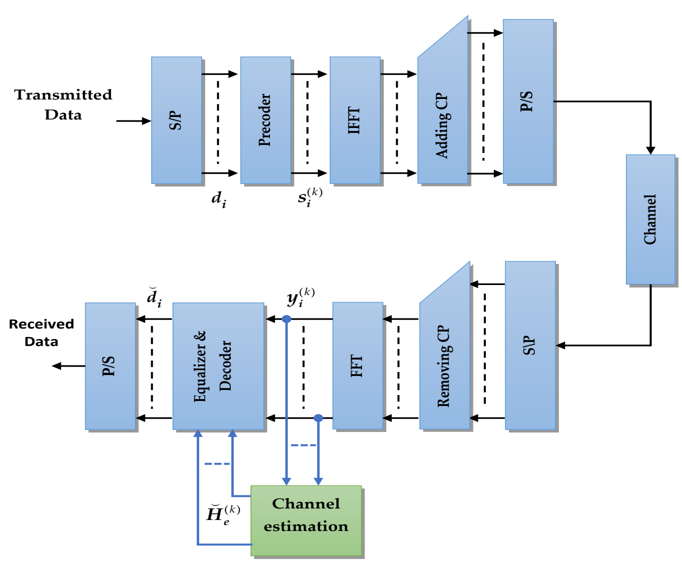

Figure 1: Block diagram of OFDM blind channel estimation

Thus, the symbols $\boldsymbol{s}_{\boldsymbol{i}}^{(k)}$ are fed into the conventional OFDM system. Assuming the channel is frequency selective, channel vector $\boldsymbol{h} = [h_0, \dots, h_L]^T$ of order $L+1$ and $h_i, i = 0, \dots, L$ are the channel coefficients in the time domain. Each transmitted block contains the CP, which is removed from each received block. It is expected that the length of the CP is longer than the channel order. The remaining signal vector at the receiver for the i-th block can be represented as:

$$\boldsymbol{y}_{\boldsymbol{i}}^{(k)} = \overline{\boldsymbol{H}}\boldsymbol{s}_{\boldsymbol{i}}^{(k)} + \boldsymbol{v}_{\boldsymbol{i}}^{(k)} = \overline{\boldsymbol{H}}\boldsymbol{A}^{(k)}\boldsymbol{d}_{\boldsymbol{i}} + \boldsymbol{v}_{\boldsymbol{i}}^{(k)} \tag{2}$$

Where $\overline{\boldsymbol{H}}$ is the matrix of channel frequency domain samples and can be expressed as $\overline{\boldsymbol{H}} = diag(\tilde{h}_0, \dots, \tilde{h}_{N-1})$ where $\tilde{h}_j, j = 0, \dots, N-1$ are the discrete Fourier transform (DFT) coefficients of the channel, $\boldsymbol{v}_{\boldsymbol{i}}^{(k)} = [v_{i,0}^{(k)}, \dots, v_{i,N-1}^{(k)}]^T$ is additive noise. We assume that noise is complex Gaussian, zero-mean, σ2-variance.

2) Blind Channel Estimation

Blind estimation in precoded OFDM systems is dependent on the structure of the autocorrelation function of the received data vectors. The auto-correlation procedures are defined as:

$$\boldsymbol{R}^{(k)} = \boldsymbol{E}\left[\boldsymbol{y}_{\boldsymbol{i}}^{(k)}\boldsymbol{y}_{\boldsymbol{i}}^{(k)\boldsymbol{H}}\right] = \left(\overline{\boldsymbol{H}}\boldsymbol{A}^{(k)}\boldsymbol{d}_{\boldsymbol{i}} + \boldsymbol{v}_{\boldsymbol{i}}^{(k)}\right)\left(\boldsymbol{d}_{\boldsymbol{i}}^{\boldsymbol{H}}\boldsymbol{A}^{(k)\boldsymbol{H}}\overline{\boldsymbol{H}}^{\boldsymbol{H}} + \boldsymbol{v}_{\boldsymbol{i}}^{(k)\boldsymbol{H}}\right)$$

$$\boldsymbol{R}^{(k)} = \overline{\boldsymbol{H}}\boldsymbol{A}^{(k)}\boldsymbol{E}\left[\boldsymbol{d}_{\boldsymbol{i}}\boldsymbol{d}_{\boldsymbol{i}}^{\boldsymbol{H}}\right]\boldsymbol{A}^{(k)\boldsymbol{H}}\overline{\boldsymbol{H}}^{\boldsymbol{H}} + \boldsymbol{E}\left[\boldsymbol{v}_{\boldsymbol{i}}^{(k)}\boldsymbol{v}_{\boldsymbol{i}}^{(k)\boldsymbol{H}}\right] \tag{3}$$

Considering the autocorrelation matrix of data and noise are:

$$\boldsymbol{E}\left[\boldsymbol{d}_{\boldsymbol{i}}\boldsymbol{d}_{\boldsymbol{i}}^{\boldsymbol{H}}\right] = \sigma^2\boldsymbol{I} = \boldsymbol{I},\ \ \boldsymbol{E}\left[\boldsymbol{v}_{\boldsymbol{i}}^{(k)}\boldsymbol{v}_{\boldsymbol{i}}^{(k)\boldsymbol{H}}\right] = \sigma_{v^{(k)}}^2\boldsymbol{I}$$

The autocorrelation matrix of received symbols can be written as:

$$\boldsymbol{R}^{(k)} = \overline{\boldsymbol{H}}\boldsymbol{P}^{(k)}\overline{\boldsymbol{H}}^{\boldsymbol{H}} + \sigma_{v^{(k)}}^2\boldsymbol{I} \tag{4}$$

Examining the first term in Equation (4), the structure is as follows::

$$\overline{\boldsymbol{H}}\boldsymbol{P}^{(k)}\overline{\boldsymbol{H}}^{\boldsymbol{H}} = \begin{bmatrix} a_{11}^{(k)}|\tilde{h}_0|^2 & a_{12}^{(k)}\tilde{h}_0\tilde{h}_1^* & \cdots & a_{1N}^{(k)}\tilde{h}_0\tilde{h}_{N-1}^* \\ a_{21}^{(k)}\tilde{h}_1\tilde{h}_0^* & a_{22}^{(k)}|\tilde{h}_1|^2 & \cdots & a_{2N}^{(k)}\tilde{h}_1\tilde{h}_{N-1}^* \\ \vdots & \vdots & \ddots & \vdots \\ a_{N1}^{(k)}\tilde{h}_{N-1}\tilde{h}_0^* & a_{N2}^{(k)}\tilde{h}_{N-1}\tilde{h}_1^* & \cdots & a_{NN}^{(k)}|\tilde{h}_{N-1}|^2 \end{bmatrix} \tag{5}$$

Where $a_{ij}^{(k)}, i, j = 1, \dots, N$ are the elements of the matrix $\boldsymbol{P}^{(k)} = \boldsymbol{A}^{(k)}\boldsymbol{A}^{(k)\boldsymbol{H}}$. The structure of matrix in (5) can be rewritten as follows:

If $\boldsymbol{H} = \left[\tilde{h}_0, \dots, \tilde{h}_{N-1}\right]^T$ is the vector containing the channel's DFT coefficients, the autocorrelation matrix of vector $\boldsymbol{H}$ can be regarded as:

$$\boldsymbol{H}\boldsymbol{H}^{\boldsymbol{H}} = \begin{bmatrix} |\tilde{h}_0|^2 & \tilde{h}_0\tilde{h}_1^* & \cdots & \tilde{h}_0\tilde{h}_{N-1}^* \\ \tilde{h}_1\tilde{h}_0^* & |\tilde{h}_1|^2 & \cdots & \tilde{h}_1\tilde{h}_{N-1}^* \\ \vdots & \vdots & \ddots & \vdots \\ \tilde{h}_{N-1}\tilde{h}_0^* & \tilde{h}_{N-1}\tilde{h}_1^* & \cdots & |\tilde{h}_{N-1}|^2 \end{bmatrix} \tag{6}$$

Using the Hadamard product (Schott, 2017) of $\boldsymbol{P}^{(k)}$ and Equation (6), we get:

$$\boldsymbol{P}^{(k)} \odot \boldsymbol{H}\boldsymbol{H}^{\boldsymbol{H}} = \begin{bmatrix} a_{11}^{(k)}\left|\tilde{h}_0\right|^2 & a_{12}^{(k)}\tilde{h}_0\tilde{h}_1^* & \cdots & a_{1N}^{(k)}\tilde{h}_0\tilde{h}_{N-1}^* \\ a_{21}^{(k)}\tilde{h}_1\tilde{h}_0^* & a_{22}^{(k)}\left|\tilde{h}_1\right|^2 & \cdots & a_{2N}^{(k)}\tilde{h}_1\tilde{h}_{N-1}^* \\ \vdots & \vdots & \ddots & \vdots \\ a_{N1}^{(k)}\tilde{h}_{N-1}\tilde{h}_0^* & a_{N2}^{(k)}\tilde{h}_{N-1}\tilde{h}_1^* & \cdots & a_{NN}^{(k)}\left|\tilde{h}_{N-1}\right|^2 \end{bmatrix} \tag{7}$$

Given that the matrix in Equation (7) and Equation (5) share the same structure, the autocorrelation matrix $\boldsymbol{R}^{(k)}$ can be written as:

$$\boldsymbol{R}^{(k)} = \boldsymbol{P}^{(k)} \odot \boldsymbol{H}\boldsymbol{H}^{\boldsymbol{H}} + \sigma_{v^{(k)}}^2\boldsymbol{I} \tag{8}$$

A new matrix is constructed by dividing both matrices (element by element) with their corresponding $\boldsymbol{P}^{(k)}$ as follows:

$$\boldsymbol{W}^{(k)} = \boldsymbol{R}^{(k)}./\boldsymbol{P}^{(k)} = \boldsymbol{H}\boldsymbol{H}^{\boldsymbol{H}} + \sigma_{\tilde{v}^{(k)}}^2\boldsymbol{I} \tag{9}$$

The normalized estimated channel vector can be calculated as follows using singular value decomposition (SVD):

$$\left[\boldsymbol{U}^{(k)}, \boldsymbol{S}^{(k)}, \boldsymbol{V}^{(k)}\right] = SVD(\boldsymbol{W}^{(k)})$$

$$\breve{\boldsymbol{H}}^{(k)} = \boldsymbol{U}^{(k)}(:,1) \tag{10}$$

Since the subspace is made up of the signal and noise vectors, the vector $\breve{\boldsymbol{H}}^{(k)}$ corresponds to the vector with the highest singular value of $\boldsymbol{U}^{(k)}$. Where $\boldsymbol{U}^{(k)}$, $\boldsymbol{V}^{(k)}$ stands for a matrix of the orthonormal vector. Due to scalar ambiguity, the vector $\breve{\boldsymbol{H}}^{(k)}$ represents the normalized estimated version of channel vector for each case of k. It can be resolved by dividing the scalar ambiguity among the constituents of the estimated vector after estimating it with a pilot symbol, as seen below:

$$Hp_m^{(k)} = \frac{1}{M}\sum_{i}^{M}\frac{y_{i,m}^{(k)}}{s_{i,m}^{(k)}} \tag{11}$$

Where M is the total number of transmitted OFDM symbols. Assuming that one pilot is placed at location m in the precoded block, $Hp_m^{(k)}$ represents the estimated channel coefficient at the subcarrier m and $s_{i,m}^{(k)}$ is the pilot symbol in the i-th block. The practical estimated channel transfer response vector $\breve{\boldsymbol{H}}_{\boldsymbol{e}}^{(k)}$ are derived as follows (Yongming et al., 2007):

$$\breve{\boldsymbol{H}}_{\boldsymbol{e}}^{(k)} = \alpha_k\breve{\boldsymbol{H}}^{(k)} \tag{12}$$

Where,

$$\alpha_k = \frac{Hp_m^{(k)}}{\breve{H}_m^{(k)}} \tag{13}$$

3) Data Detection

After the channel has been estimated, and since we are not concerned with data estimation methods, a simple zero-forcing solution is implemented for symbol detection.

$$\breve{\boldsymbol{d}}_{\boldsymbol{i}}^{(k)} = \left(\breve{\boldsymbol{H}}_{\boldsymbol{d}}^{(k)} \boldsymbol{A}^{(k)}\right)^{-\mathbf{1}} \boldsymbol{y}_{\boldsymbol{i}}^{(k)} \tag{14}$$

Where $\breve{\boldsymbol{d}}_{\boldsymbol{i}}^{(k)}$ are the estimated data vectors and $\breve{\boldsymbol{H}}_{\boldsymbol{d}}^{(k)} = diag\left(\breve{\boldsymbol{H}}_{\boldsymbol{e}}^{(k)}\right)$ is the diagonal matrix of the estimated channel frequency impulse response.

3 OFDM Channel Estimation with a Block Precoding Matrix

1) System Model

In this model, we precode every pair of adjacent symbols, and then the precoding matrix is made up of blocks of four matrices as follows:

The data stream blocks are defined as a block version with $\boldsymbol{D}_{\boldsymbol{i}} = [\boldsymbol{d}_{\boldsymbol{2i}} \quad \boldsymbol{d}_{\boldsymbol{2i+1}}]^T$, where $\boldsymbol{d}_{\boldsymbol{2i}}$ and $\boldsymbol{d}_{\boldsymbol{2i+1}}$ are the even and odd data blocks of the data stream, respectively, with the same assumptions as the previous model. Next, the conveyed symbols are stated as:

$$\boldsymbol{S}_{\boldsymbol{i}}^{(k)} = \begin{bmatrix} \boldsymbol{s}_{\boldsymbol{2i}}^{(k)} \\ \boldsymbol{s}_{\boldsymbol{2i+1}}^{(k)} \end{bmatrix} = \begin{bmatrix} \boldsymbol{A}_{\boldsymbol{11}}^{(k)} & \boldsymbol{A}_{\boldsymbol{12}}^{(k)} \\ \boldsymbol{A}_{\boldsymbol{21}}^{(k)} & \boldsymbol{A}_{\boldsymbol{22}}^{(k)} \end{bmatrix} \begin{bmatrix} \boldsymbol{d}_{\boldsymbol{2i}} \\ \boldsymbol{d}_{\boldsymbol{2i+1}} \end{bmatrix} = \boldsymbol{A}_{\boldsymbol{b}}^{(k)} \boldsymbol{D}_{\boldsymbol{i}} \tag{15}$$

Where $\boldsymbol{S}_{\boldsymbol{i}}^{(k)} = \left[\boldsymbol{s}_{\boldsymbol{2i}}^{(k)} \quad \boldsymbol{s}_{\boldsymbol{2i+1}}^{(k)}\right]^T$ is the modulate symbol block vector, and $\boldsymbol{A}_{\boldsymbol{b}}^{(k)}$ of size $2N \times 2N$ is the block precoding matrix. The received signal block can be represented as:

$$\boldsymbol{Y}_{\boldsymbol{i}}^{(k)} = \begin{bmatrix} \boldsymbol{y}_{\boldsymbol{2i}}^{(k)} \\ \boldsymbol{y}_{\boldsymbol{2i+1}}^{(k)} \end{bmatrix} = \begin{bmatrix} \overline{\boldsymbol{H}} & \boldsymbol{0} \\ \boldsymbol{0} & \overline{\boldsymbol{H}} \end{bmatrix} \begin{bmatrix} \boldsymbol{A}_{\boldsymbol{11}}^{(k)} & \boldsymbol{A}_{\boldsymbol{12}}^{(k)} \\ \boldsymbol{A}_{\boldsymbol{21}}^{(k)} & \boldsymbol{A}_{\boldsymbol{22}}^{(k)} \end{bmatrix} \begin{bmatrix} \boldsymbol{d}_{\boldsymbol{2i}} \\ \boldsymbol{d}_{\boldsymbol{2i+1}} \end{bmatrix} + \begin{bmatrix} \boldsymbol{v}_{\boldsymbol{2i}}^{(k)} \\ \boldsymbol{v}_{\boldsymbol{2i+1}}^{(k)} \end{bmatrix}$$

$$\boldsymbol{Y}_{\boldsymbol{i}}^{(k)} = \overline{\overline{\boldsymbol{H}}} \boldsymbol{A}_{\boldsymbol{b}}^{(k)} \boldsymbol{D}_{\boldsymbol{i}} + \boldsymbol{V}_{\boldsymbol{i}}^{(k)} \tag{16}$$

Where $\overline{\overline{\boldsymbol{H}}} = diag([\overline{\boldsymbol{H}} \quad \overline{\boldsymbol{H}}])$ and and $\overline{\boldsymbol{H}} = diag\left(\tilde{h}_0, \ldots, \tilde{h}_{N-1}\right)$, where $\tilde{h}_j$ are the DFT coefficients of the channel in the prior model and $\boldsymbol{A}_{\boldsymbol{b}}^{(k)}$ is the blocked version of the matrices $\left(\boldsymbol{A}_{\boldsymbol{11}}^{(k)}, \boldsymbol{A}_{\boldsymbol{12}}^{(k)}, \boldsymbol{A}_{\boldsymbol{21}}^{(k)}, \boldsymbol{A}_{\boldsymbol{22}}^{(k)}\right)$, $\boldsymbol{V}_{\boldsymbol{i}}^{(k)} = \left[\boldsymbol{v}_{\boldsymbol{2i}}^{(k)} \quad \boldsymbol{v}_{\boldsymbol{2i+1}}^{(k)}\right]^T$ is the additive noise vector. Given that the method depends on the relationship between each pair of adjacent symbols, the symbols that are received can be described as:

$$\boldsymbol{y}_{\boldsymbol{2i}}^{(k)} = \overline{\boldsymbol{H}} \left(\boldsymbol{A}_{\boldsymbol{11}}^{(k)} \boldsymbol{d}_{\boldsymbol{2i}} + \boldsymbol{A}_{\boldsymbol{12}}^{(k)} \boldsymbol{d}_{\boldsymbol{2i+1}}\right) + \boldsymbol{v}_{\boldsymbol{2i}}^{(k)} \tag{17}$$

$$\boldsymbol{y}_{\boldsymbol{2i+1}}^{(k)} = \overline{\boldsymbol{H}} \left(\boldsymbol{A}_{\boldsymbol{21}}^{(k)} \boldsymbol{d}_{\boldsymbol{2i}} + \boldsymbol{A}_{\boldsymbol{22}}^{(k)} \boldsymbol{d}_{\boldsymbol{2i+1}}\right) + \boldsymbol{v}_{\boldsymbol{2i+1}}^{(k)} \tag{18}$$

2) Blind Channel Estimation

The cross-correlation of two consecutive symbols is forced by the precoding system's structure to produce a unique formation as follows:

$$\boldsymbol{R}^{(k)} = \boldsymbol{E}\left[\boldsymbol{y}_{2i}^{(k)}\boldsymbol{y}_{2i+1}^{(k)\boldsymbol{H}}\right]$$

$$\boldsymbol{R}^{(k)} = \boldsymbol{E}\left[\left(\overline{\boldsymbol{H}}\left(\boldsymbol{A}_{11}^{(k)}\boldsymbol{d}_{2i} + \boldsymbol{A}_{12}^{(k)}\boldsymbol{d}_{2i+1}\right) + \boldsymbol{v}_{2i}^{(k)}\right)\left(\left(\boldsymbol{d}_{2i}^{\boldsymbol{H}}\boldsymbol{A}_{21}^{(k)\boldsymbol{H}} + \boldsymbol{d}_{2i+1}^{\boldsymbol{H}}\boldsymbol{A}_{22}^{(k)\boldsymbol{H}}\right)\overline{\boldsymbol{H}}^{\boldsymbol{H}} + \boldsymbol{v}_{2i+1}^{(k)\boldsymbol{H}}\right)\right] \tag{19}$$

The preceding equation can be reduced to the following values because of the properties of data blocks and noise vectors:

$$\boldsymbol{R}^{(k)} = \boldsymbol{E}\left[\overline{\boldsymbol{H}}\left(\boldsymbol{A}_{11}^{(k)}\boldsymbol{d}_{2i} + \boldsymbol{A}_{12}^{(k)}\boldsymbol{d}_{2i+1}\right)\left(\boldsymbol{d}_{2i}^{\boldsymbol{H}}\boldsymbol{A}_{21}^{(k)\boldsymbol{H}} + \boldsymbol{d}_{2i+1}^{\boldsymbol{H}}\boldsymbol{A}_{22}^{(k)\boldsymbol{H}}\right)\overline{\boldsymbol{H}}^{\boldsymbol{H}}\right] + \boldsymbol{E}\left[\boldsymbol{v}_{2i}^{(k)}\boldsymbol{v}_{2i+1}^{(k)\boldsymbol{H}}\right] \tag{20}$$

$$\boldsymbol{R}^{(k)} = \overline{\boldsymbol{H}}\left(\boldsymbol{A}_{11}^{(k)}\boldsymbol{A}_{21}^{(k)\boldsymbol{H}} + \boldsymbol{A}_{12}^{(k)}\boldsymbol{A}_{22}^{(k)\boldsymbol{H}}\right)\overline{\boldsymbol{H}}^{\boldsymbol{H}}$$

$$\boldsymbol{R}^{(k)} = \overline{\boldsymbol{H}}\boldsymbol{P}^{(k)}\overline{\boldsymbol{H}}^{\boldsymbol{H}} \tag{21}$$

Equation (21) revealed that the cross correlation's structure is comparable to the term in Equation (5), $\boldsymbol{R}^{(k)}$, and as a result, it can be expressed as:

$$\boldsymbol{R}^{(k)} = \boldsymbol{P}^{(k)} \odot \boldsymbol{H}\boldsymbol{H}^{\boldsymbol{H}} \tag{22}$$

Where $\boldsymbol{H}$ is already defined in the previous model. A new matrix is constructed by dividing both matrices element by element with their corresponding $\boldsymbol{P}^{(k)}$ as follows:

$$\boldsymbol{W}^{(k)} = \boldsymbol{R}^{(k)}./\boldsymbol{P}^{(k)} = \boldsymbol{H}\boldsymbol{H}^{\boldsymbol{H}} \tag{23}$$

The remaining steps are as mentioned in the first model, where SVD was implemented and the scalar ambiguity was removed with a pilot signal. The estimated channel vector is then denoted as $\breve{\boldsymbol{H}}_{\boldsymbol{e}}^{(k)}$. Numerous research have looked at this OFDM system with a blocked precoding matrix (Liang, Luo, Xu, & Huang, 2006; Rui Lin & Petropulu, 2003; Shengli Zhou, Muquet, & Giannakis, 2002), and the main advantage of this type is the reduced number of operations that must be performed to obtain the correlation matrix, which is reduced to half compared to the first model.

3) Data Detection

As described in the preceding model, a simple zero-force solution is used for symbol detection.

$$\breve{\boldsymbol{D}}_{\boldsymbol{i}}^{(k)} = \left(\breve{\boldsymbol{H}}_{\boldsymbol{d}}^{(k)}\boldsymbol{A}_{\boldsymbol{b}}^{(k)}\right)^{-\boldsymbol{1}}\boldsymbol{Y}_{\boldsymbol{i}}^{(k)} \tag{24}$$

Where $\breve{\boldsymbol{D}}_{\boldsymbol{i}}^{(k)}$ is the estimated data vectors and $\breve{\boldsymbol{H}}_{\boldsymbol{d}}^{(k)} = diag\left(\left[\breve{\boldsymbol{H}}_{\boldsymbol{e}}^{(k)} \quad \breve{\boldsymbol{H}}_{\boldsymbol{e}}^{(k)}\right]^T\right)$.

4 Precoding Matrix Design

Generally speaking, the precoder needs to meet the following crucial requirements (Lin & Petropulu, 2005; Rui Lin & Petropulu, 2003):

1. Full rank property must be maintained in the precoder matrix, which can be accomplished by creating a particular precoding matrix structure.
2. The precoder has to keep the symbol's average power constant. In other words:

$$\boldsymbol{E}\left[\left\|\boldsymbol{A}^{(k)}\boldsymbol{d_i}\right\|^{\boldsymbol{2}}\right] = tr\left(\boldsymbol{E}\left[\boldsymbol{A}^{(k)}\boldsymbol{d_i}\boldsymbol{d_i^H}\boldsymbol{A}^{(k)\boldsymbol{H}}\right]\right) \leq \boldsymbol{E}\left[\|\boldsymbol{d_i}\|^{\boldsymbol{2}}\right] \tag{25}$$

1) Circulant Precoder $\boldsymbol{A}^{(\boldsymbol{1})}$

This type of precoding matrix has been used in numerous studies for OFDM channel estimation (Liang et al., 2006; Ruifeng Zhang, n.d.). Equation (26) shows the structure of the precoding matrix.

With this precoding matrix, the first need is met, and to some extent, the second requirement can be met as well by choosing the value of ρ.

$$\boldsymbol{A}^{(1)} = \begin{bmatrix} \sqrt{\rho} & \sqrt{\frac{1-\rho}{N-1}} & \cdots & \sqrt{\frac{1-\rho}{N-1}} \\ \sqrt{\frac{1-\rho}{N-1}} & \sqrt{\rho} & \cdots & \sqrt{\frac{1-\rho}{N-1}} \\ \vdots & \vdots & \ddots & \vdots \\ \sqrt{\frac{1-\rho}{N-1}} & \sqrt{\frac{1-\rho}{N-1}} & \cdots & \sqrt{\rho} \end{bmatrix} \tag{26}$$

Where $0 < \rho < 1$. The matrix $\boldsymbol{P}^{(k)}$ has a special design as:

$$\boldsymbol{P}^{(1)} = \boldsymbol{A}^{(1)}\boldsymbol{A}^{(1)H} = \begin{bmatrix} 1 & q & \cdots & q \\ q & 1 & \cdots & q \\ \vdots & \vdots & \ddots & \vdots \\ q & q & \cdots & 1 \end{bmatrix} \tag{27}$$

Where, $q = 2\sqrt{(\rho(1-\rho)/((N-1)\,))} + (1-\rho)(N-2)/((N-1)\,)$.

The SNR loss due to the precoder can also be controlled by the parameter ρ. Equation (26) stands for the precoding matrix from the first model. The second model's precoding matrix is structured as follows:

$$\boldsymbol{A_b}^{(1)} = \begin{bmatrix} \boldsymbol{A_{11}^{(1)}} & \boldsymbol{A_{12}^{(1)}} \\ \boldsymbol{A_{21}^{(1)}} & \boldsymbol{A_{22}^{(1)}} \end{bmatrix} \tag{28}$$

We select the blocked matrix's structure in accordance with (Liang et al., 2006; Ruifeng Zhang, n.d.) as follows:

$$\boldsymbol{A_{11}^{(1)}} = \boldsymbol{A_{22}^{(1)}} = \frac{2}{3}\boldsymbol{A}^{(1)} \tag{29}$$

$$\boldsymbol{A_{12}^{(1)}} = \boldsymbol{A_{21}^{(1)}} = \frac{1}{3}\boldsymbol{A}^{(1)} \tag{30}$$

This matrix is used in the first case of precoding matrix of the second model.

2) Design of SVD-Based Symmetric Precoder

We propose a new precoder design that can be created with the Toeplitz function and an exponentially decaying function. First we define a vector $\boldsymbol{r}$ of length N, the elements of such vector can be obtained by Equation (31).

$$\boldsymbol{r} = [r(1), r(2), \ldots, r(N)]$$

$$r(i) = 2\rho e^{\left(-2\rho\frac{i-1}{N}\right)}, \quad i = 1, \ldots, N \tag{31}$$

Then by deploying Toeplitz function we generate a symmetric matrix $\boldsymbol{A_T}$ as following:

$$\boldsymbol{A_T} = Toeplitz\left(\boldsymbol{r}, \boldsymbol{r^T}\right) \tag{32}$$

By using SVD for $\boldsymbol{A_T}$, the final precoding matrix has been constructed as follows:

$$\boldsymbol{A_f} = \boldsymbol{U} \times \boldsymbol{S} \tag{33}$$

Where $\boldsymbol{U}$ is the matrix of orthonormal vectors and $\boldsymbol{S}$ is a diagonal matrix of the singular values of SVD.

3) SVD-based Circulant Precoder

Another method of generating SVD-based precoders can be presented as in (Al-Qadhi, Semenov, et al., 2024; Al-Qadhi et al., 2023) using the vector definition in Equation (34).

$$r_W(i) = \begin{cases} 2\rho e^{\left(-2\rho\frac{i-1}{N}\right)} & \rho > 0 \quad for\, \frac{i-1}{W} \in \mathbb{Z} \\ \frac{1}{\sqrt{N}} & otherwise \end{cases} \tag{34}$$

Where $r_W(i)$ are the elements of the row vector $\boldsymbol{r_W}$ and w is an integer and defined between [1, N]. The two precoding matrices $\boldsymbol{A}^{(2)}$ and $\boldsymbol{A}^{(3)}$ are designed as follows:

1. Generate two row vectors $\boldsymbol{r_N}$ and $\boldsymbol{r_{N/4}}$ according to Equation (34).
2. Construct the corresponding Circulant matrix $A_T^{(l)}$ as in Equation (35).

$$\boldsymbol{A_T^{(l)}} = Toeplitz\left(\left[r_{W_l}(1) \quad flip\left(r_{W_l}(2{:}\,N)\right)\right], \boldsymbol{r_{W_l}^T}\right) \tag{35}$$

Where l = 2,3, $W_2 = N$, $W_3 = N/4$.

3. Utilizing SVD for $\boldsymbol{A_T^{(l)}}$is the last step to obtain the final matrix. After that, we may build the matrix as follows:

$$\left[\boldsymbol{U}^{(l)}, \boldsymbol{S}^{(l)}, \boldsymbol{V}^{(l)}\right] = \mathrm{SVD}\left(\boldsymbol{A_T^{(l)}}\right) \tag{36}$$

$$\boldsymbol{A}^{(l)} = \boldsymbol{U}^{(l)} \times \boldsymbol{S}^{(l)} \tag{37}$$

We propose that the value of ρ be positive since we don’t want to introduce any phase values to the systems where the upper limit can be determined by the average signal power of the system.

The design of both $\boldsymbol{A_b^{(2)}}$ and $\boldsymbol{A_b^{(3)}}$ following the Equations (34), (35), (36) and (37), considering that $\boldsymbol{A}^{(2)}$ and $\boldsymbol{A}^{(3)}$ as the element of the final matrices. Appendix A established that the matrix $\boldsymbol{A}^{(2)}$ has full rank property because it shares the same general structure as $\boldsymbol{A}^{(1)}$. A similar proof for the rank property of matrix $\boldsymbol{A}^{(3)}$ for w = N / 4 is mentioned in Appendix B.

5 Results

We investigate the effectiveness of the suggested estimator in multiple scenarios, utilizing the exponential power delay profile channel model (Al-Qadhi, Abdul-Rahaim, et al., 2024; Al-Qadhi, Semenov, et al., 2024; Al-Qadhi et al., 2023):

$$E[\|h_l\|^2] = exp\left(-\frac{l}{\tau_{rms}/T_s}\right), l = 0, \dots, L_c \tag{38}$$

The Naftali model is applied to this channel (Dou & Wang, 2010) as follows:

$$h_l(k) = N\left(0, \frac{1}{2}\sigma_l^2\right) + jN\left(0, \frac{1}{2}\sigma_l^2\right), k = 1, \dots, n, l = 0, \dots, L_c \tag{39}$$

Where $N(0{,}0.5\sigma_l^2)$ represents a Gaussian random variable characterized by a zero-mean and a variance of $0.5\sigma_l^2$, where denotes the expected value of the norm squared of the channel impulse $\sigma_l^2 = E[\|h_l\|^2]$, n corresponds to the total number of realizations of the generated channel impulse response. The channel model parameters are $\tau_{rms}/T_s = 10$, $n = 40$. The OFDM parameter of the simulation was chosen as follows: $N = 64$, $CP = 16$, modulation type is 16QAM and $L_c = 2$. Utilizing a Monte-Carlo run $n_w = 160$, the simulation was executed with various numbers of OFDM symbols.

The normalized estimate mean square errors of the channel (NMSE) can be computed using the following formula:

$$NMSE(k) = \frac{1}{n \times n_w} \sum_{i}^{n_w} \sum_{j}^{n} \frac{var\left(\boldsymbol{H}_{(j)} - (\breve{\boldsymbol{H}}_{\boldsymbol{e}}^{(k)})_{(i,j)}\right)}{var\left(\boldsymbol{H}_{(j)}\right)} \tag{40}$$

Where i is the Monte-Carlo run index and j is the channel realization index. We first create channel realizations, then we use the created channel vectors to estimate each case for each individual Monte Carlo run, and finally we apply NMSE as in Equation (40). In this paper, we investigate several scenarios, as follows:

Scenario 1

In Figure 2, we examine the proposed single precoding matrix $\boldsymbol{A_f}$ using first model, and contrasted it with the circulant precoding matrix $\boldsymbol{A}^{(1)}$.

In this scenario, it is clear that $\boldsymbol{A_f}$ performs better than all other curves at both ($\rho = 0.1$ and $\rho = 0.3$), and that when SNR increases, and that the gap between curves increases in favor of the matrix $\boldsymbol{A_f}$ up to a specific point as SNR increases.

Figure 3 illustrates the drawbacks of utilizing $\boldsymbol{A_f}$, as its BER performance is consistently lower than that of $\boldsymbol{A}^{(1)}$ for all values of ρ. Since the inverse of $\boldsymbol{A_f}$, affects BER, which has to reduce the impact of noise vector on the data estimate, the data detection method must be improved in order to employ this kind of precoder in applications where data detection is necessary.

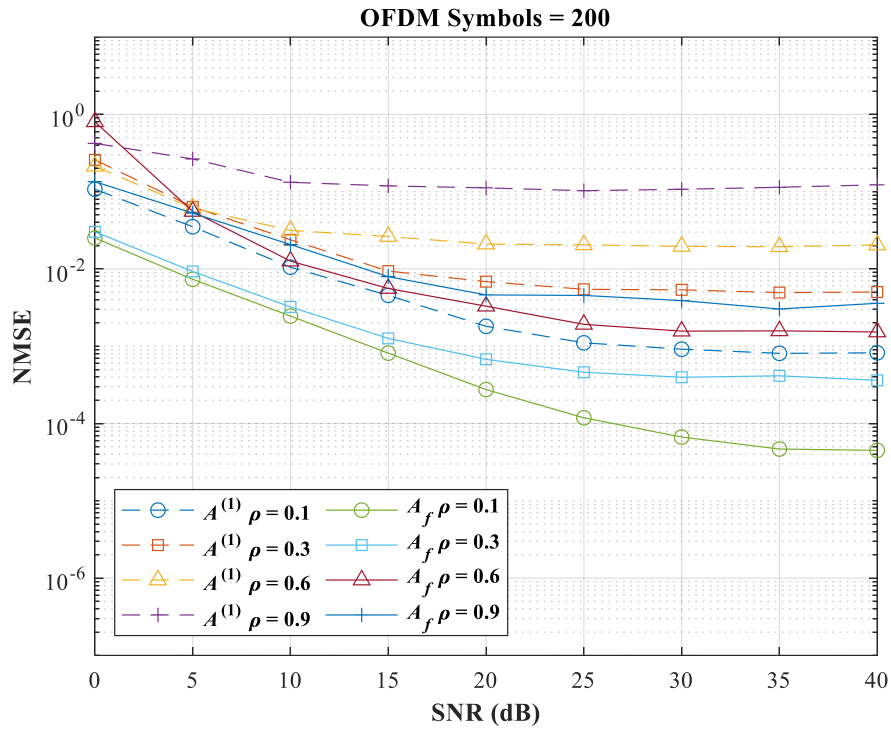

Figure 2: NMSE for the first proposed matrix

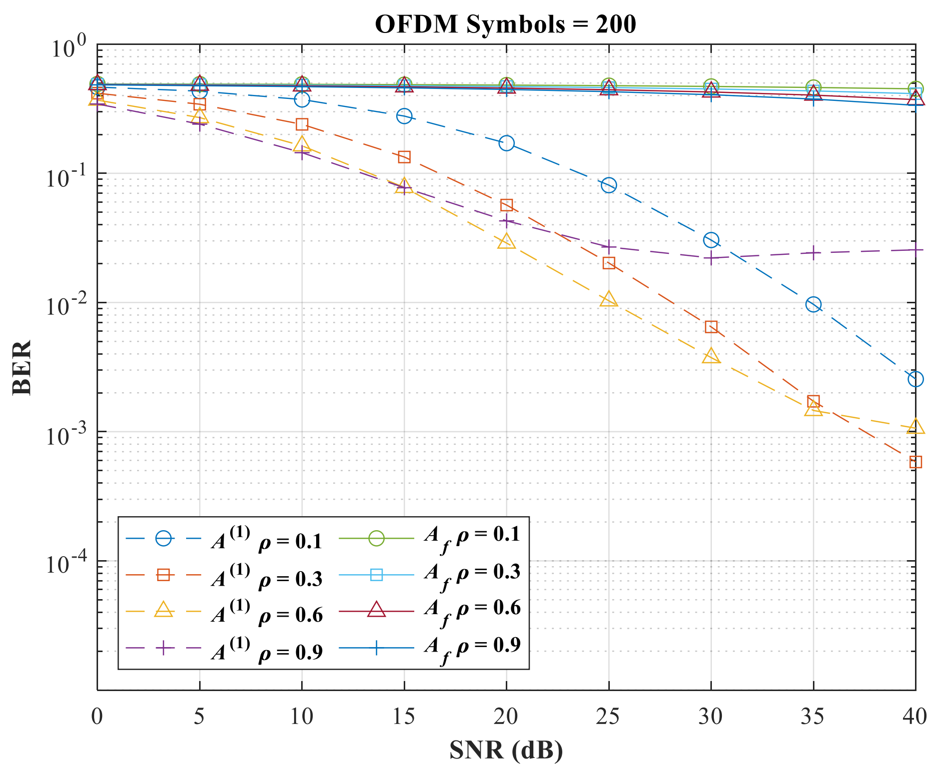

Figure 3: BER for the first proposed matrix

Scenario 2

In this case, we investigate the proposed OFDM system's channel estimate utilizing matrices $\boldsymbol{A}^{(2)}$ and $\boldsymbol{A}^{(3)}$. The matrices $\boldsymbol{A}^{(2)}$ and $\boldsymbol{A}^{(3)}$ at $\rho = 0.1$ outperform other curves in terms of NMSE, as seen in Figure 4.

Results for the same ρ value for $\rho = 0.3,0.6$ varied slightly from the previous instance. Even at larger ρ values, the suggested technique outperforms the other two matrices in both scenarios..

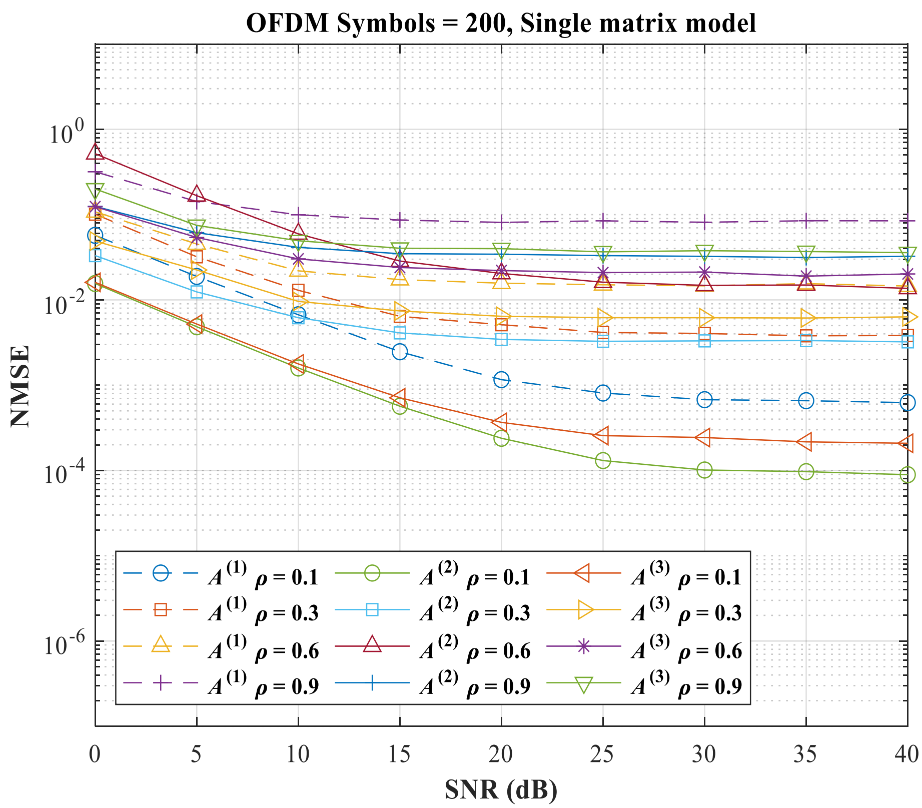

Figure 4: NMSE for the single matrix model at lower OFDM symbols

Figure 5 summarizes the BER and shows that, at the same ρ value, the curves of $\boldsymbol{A}^{(1)}$ are superior to the curves of $\boldsymbol{A}^{(3)}$, except for a greater SNR (corresponding to distinct SNR values for each case of ρ).

$\boldsymbol{A}^{(2)}$ works better for higher SNR values as the distance between the curves expands, while $\boldsymbol{A}^{(1)}$ performs slightly better at lower SNR (SNR < 20dB with $\rho = 0.9$, SNR < 30dB with $\rho = 0.6$, and SNR < 35dB with $\rho = 0.3$). The BER performance of $\boldsymbol{A}^{(2)}$ at $\rho = 0.1$ is lower than the corresponding ρ value of $\boldsymbol{A}^{(1)}$. In contrast to $\boldsymbol{A}^{(1)}$, the curves of $\boldsymbol{A}^{(2)}$ are proportional to SNR and lack a defined zone.

Scenario 3

In this case, we investigate the proposed OFDM system's channel estimate utilizing matrices $\boldsymbol{A}_{\boldsymbol{b}}^{(2)}$ and $\boldsymbol{A}_{\boldsymbol{b}}^{(3)}$.

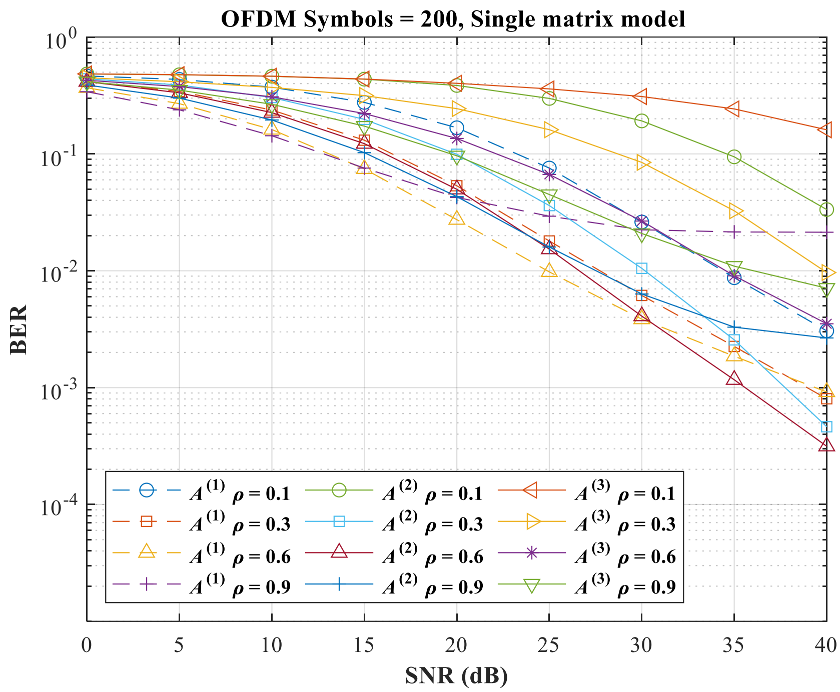

Figure 5: BER for the single matrix model at lower OFDM symbols

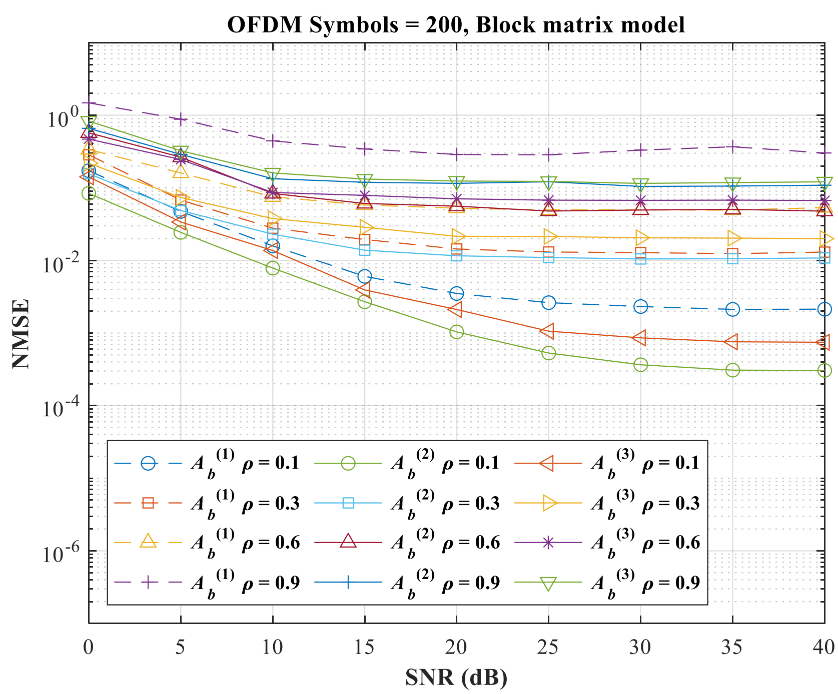

Figure 6: NMSE for the block matrix model at lower OFDM symbols

As a comparison between the SVD-Based block matrices ($\boldsymbol{A}_{\boldsymbol{b}}^{(2)}$, $\boldsymbol{A}_{\boldsymbol{b}}^{(3)}$) and the circulant block matrix $\boldsymbol{A}_{\boldsymbol{b}}^{(1)}$, the NMSE result in Figure 6 demonstrates the same behavior, demonstrating that the overall findings are the same as the prior model with different intersection locations.

Figure 7 indicates that using $\boldsymbol{A}_{\boldsymbol{b}}^{(1)}$ improves BER performance compared to $\boldsymbol{A}_{\boldsymbol{b}}^{(2)}$ and $\boldsymbol{A}_{\boldsymbol{b}}^{(3)}$ for the same ρ value, except for higher SNR, when $\boldsymbol{A}_{\boldsymbol{b}}^{(2)}$ displays a better BER after 35dB SNR.

Additionally, it is observed that, in contrast to the previous scenario, the curves of the proposed matrices enter a fixed value zone at different SNR values. This behavior is primarily caused by the fact that, for an equivalent number of OFDM symbols, the number of cross-correlation matrix calculations in the second system is half that of the autocorrelation in the first system.

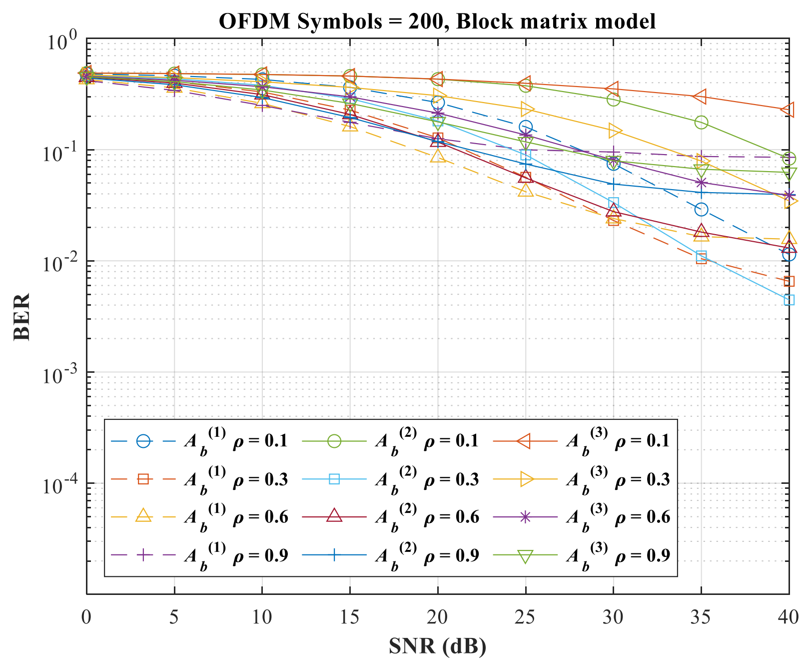

Figure 7: BER for the block matrix model at lower OFDM symbols

Scenario 4

We contrast the outcomes of the two system models in this case. By comparing the curves representing the best NMSE performance for the two system models with the best performance obtained using the subspace methods in (Al-Qadhi, Abdul-Rahaim, et al., 2024), Figure 8 enables us to illustrate the advantages of using precoding matrices with different values of ρ.

With the exception of $\boldsymbol{A}_{\boldsymbol{b}}^{(1)}$ with $\rho = 0.1$ at SNR > 27dB, where the Zero padding approach performs better, all NMSE curves perform better overall than the subspace method. It can be observed that $\boldsymbol{A}_{\boldsymbol{f}}$ performs best at higher SNR values (over 25 dB), while $\boldsymbol{A}^{(2)}$ performs better at lower SNR values.

Given the influence of the number of OFDM symbols on the estimated results, we conducted an analysis to observe the alterations in the most optimal curves in relation to NMSE curves. Figure 9 presented the results of the analysis for both systems, accounting for the various amounts of OFDM symbols present and the different SNR values at lower and higher levels.

It is shown that the best performance at lower SNR is achieved by using $\boldsymbol{A}^{(2)}$ or $\boldsymbol{A}^{(3)}$ at $\rho = 0.1$ in the first system and $\boldsymbol{A}^{(2)}$ with $\rho = 0.1$ at higher SNR. Since BER results demonstrate distinct behaviors of the precoding matrices, it is relevant examining BER performance vs. the number of OFDM symbols.

Figure 10 shows two distinct SNR scenarios: at lower SNR, all systems behave identically, and the number of OFDM symbols changes without causing any changes. As the number of OFDM symbols increases, matrix $\boldsymbol{A}^{(2)}$ performs better for larger SNR.

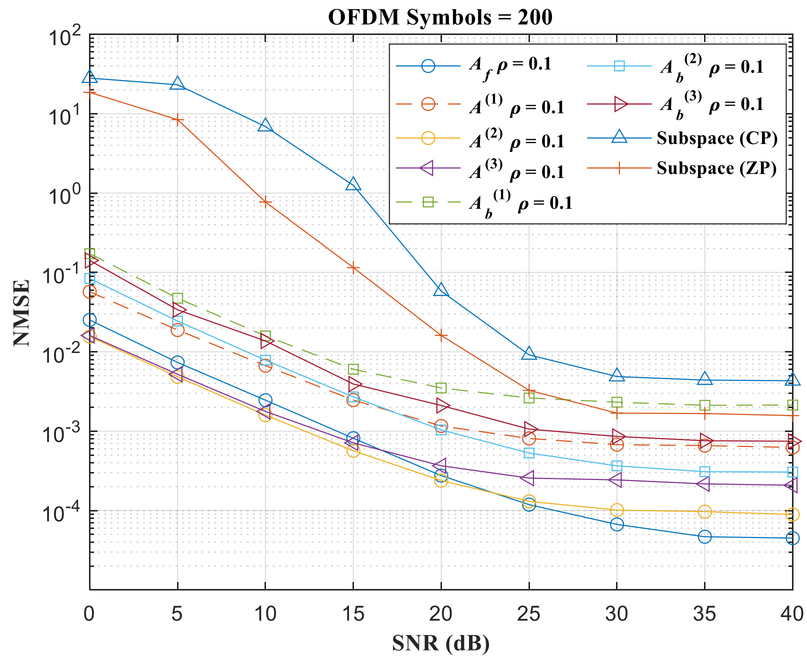

Figure 8: Comparing the NMSE of the two models with the best-performing curves

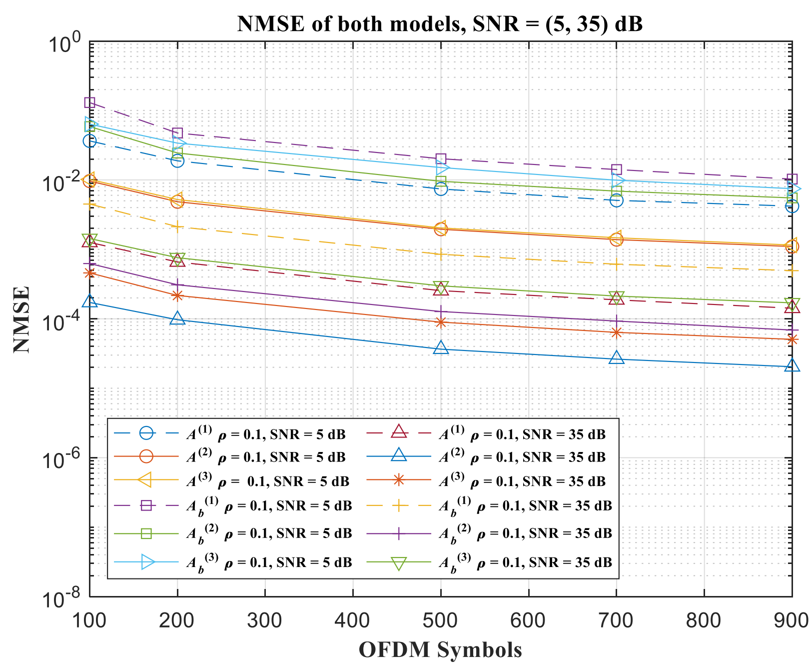

Figure 9: NMSE comparison of both models vs number of OFDM symbols

In Figure 11, a similar observation of the lower SNR and the best performance is shown, where using $\boldsymbol{A}^{(2)}$ at higher SNR shows the best performance over all results, where the gap between the curves is almost fixed with increase in the number of OFDM symbols.

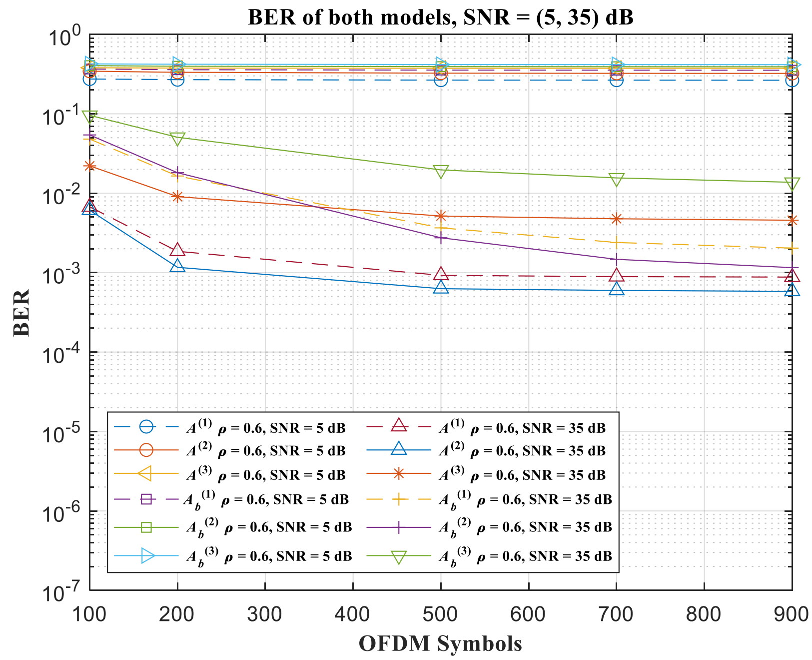

Figure 10: BER comparison of both models vs number of OFDM symbols with $\rho = 0.6$

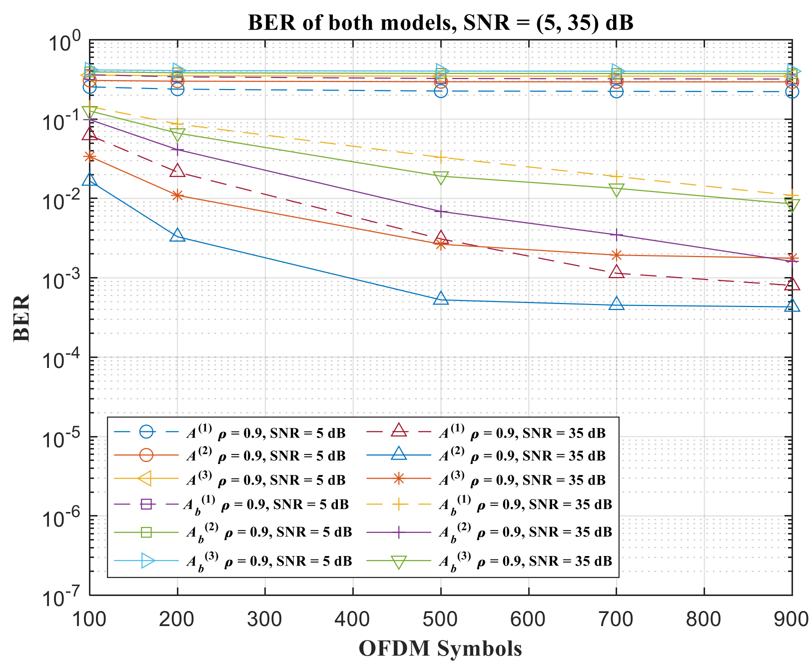

Figure 11: BER comparison of both models vs number of OFDM symbols with $\rho = 0.9$

Figure 12 illustrates the impact of precoders on the average power of transmitted symbols. This illustrates how, depending on the system requirements, implementing the suggested precoder can affect power in either direction (increasing or lowering).

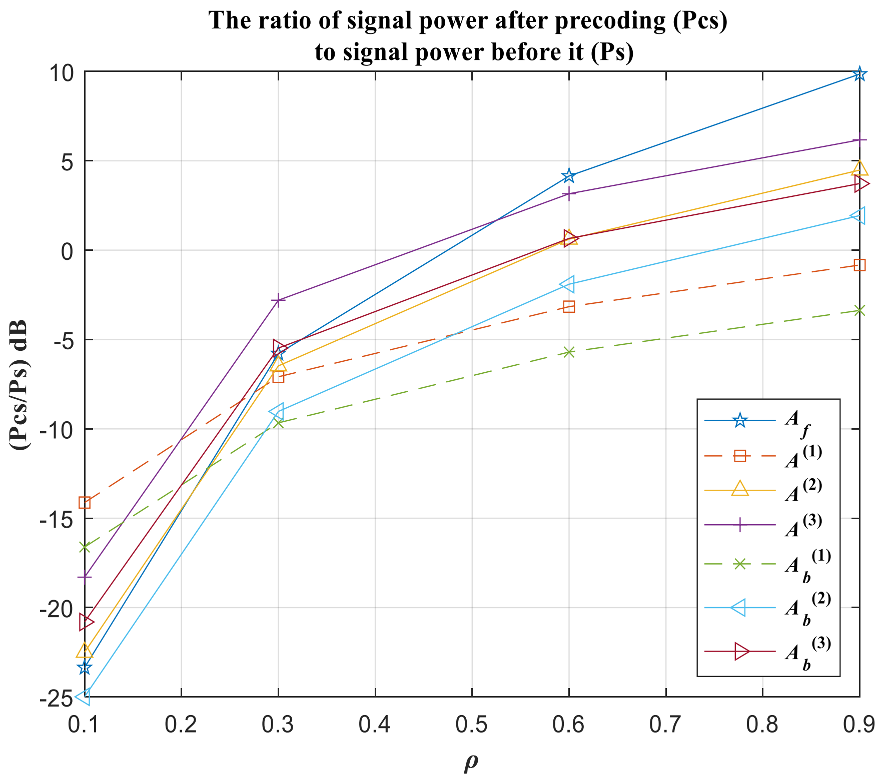

Figure 12: Relative average signal power before (Ps) and after (Pcs) precoding

6 Conclusion

In this work, a new precoding matrix design for blind channel estimation in OFDM systems based on SVD is presented. The new design is examined and simulated within an OFDM system using a cyclic prefix as a guard interval. The NMSE and BER results are compared with those of the circulant precoding matrix and other SVD-based precoding matrix. The results were analyzed for various SNR, OFDM symbol, and ρ values under the same channel conditions. Compared to a typical circulant precoder, an SVD-based precoder has several advantages, including the ability to regulate signal power and provide multiple precoding matrix versions. The benefits of utilizing this strategy are demonstrated by comparing the NMSE results for subspace and precoding methods. Since knowledge of the channel vector affects the BER, the primary use of this method is to solve the multipath issue.

A new precoding matrix can be designed more easily when certain prerequisites are met, as demonstrated by the precoding matrix's proof of rank property. This precoding matrix can be used with zero-padding and other forms of OFDM systems, particularly in applications where channel identification is necessary.

Appendix A

Proving the full-rank property of circulant matrix $\boldsymbol{A}^{(1)}$ (Al-Qadhi, Semenov, et al., 2024) is as follows:-

If the matrix $\boldsymbol{A}^{(1)}$ is a full rank, the matrix $\boldsymbol{A}_{\boldsymbol{T}}^{(1)}$ is likewise a full rank (since they share the same structure), and the vectors representing its columns are linearly independent. This means that if the vector $\boldsymbol{\beta} \in \mathbb{R}^N$, $\boldsymbol{\beta} = [\beta_1, \beta_2, \ldots, \beta_N]^T$, then:

If $\boldsymbol{A}_{\boldsymbol{T}}^{(1)}\boldsymbol{\beta} = \mathbf{0}$, $\boldsymbol{A}_{\boldsymbol{T}}^{(1)}$ is of full rank, then $\boldsymbol{\beta} = \mathbf{0}$, which indicates $\beta_i = 0$ for $i = 1,2, \ldots, N-1, N$ where $\beta_i \in \boldsymbol{\beta}$.

In the next steps, we verify the full rank property of $\boldsymbol{A}_{\boldsymbol{T}}^{(1)}$, whose structure is presented below.

$$\boldsymbol{A}_{\boldsymbol{T}}^{(1)} = \begin{bmatrix} x & y & \cdots & y \\ y & x & \cdots & \vdots \\ \vdots & \vdots & \ddots & \vdots \\ y & \cdots & \cdots & x \end{bmatrix} \tag{41}$$

Where $x = \sqrt{\rho}$, $y = \sqrt{\frac{1-\rho}{N-1}}$. Assuming that the vector $\boldsymbol{\beta} \neq \mathbf{0}$, then $\boldsymbol{A}_{\boldsymbol{T}}^{(1)}\boldsymbol{\beta}$ can be viewed as follows:

$$\boldsymbol{A}_{\boldsymbol{T}}^{(1)}\boldsymbol{\beta} = \begin{bmatrix} x & y & \cdots & y \\ y & x & \cdots & \vdots \\ \vdots & \vdots & \ddots & \vdots \\ y & \cdots & \cdots & x \end{bmatrix} \begin{bmatrix} \beta_1 \\ \beta_2 \\ \vdots \\ \beta_N \end{bmatrix} = \begin{bmatrix} 0 \\ 0 \\ \vdots \\ 0 \end{bmatrix} \tag{42}$$

N equations can be constructed in the following ways:

Row #1
$$\beta_1 x + \sum_{i=2}^{N} \beta_i y = 0 \tag{43}$$

Row #2
$$\beta_2 x + \sum_{i=2}^{N} \beta_i y = 0 \tag{44}$$

The general form for any row # j is written as follows:

Row # j
$$\beta_j x + \sum_{(i=1),(i\neq j)}^{N} \beta_i y = 0 \tag{45}$$

Adding together the N row equations gives us the following:

$$x \sum_{j=1}^{N} \beta_j + y \sum_{j=1}^{N} \left(\sum_{(i=1),(i\neq j)}^{N} \beta_i \right) = 0 \tag{46}$$

Expanding the second term in Equation (46) uncovers the following common elements:

$$\sum_{j=1}^{N} \left(\sum_{(i=1),(i\neq j)}^{N} \beta_i \right) = (\beta_2 + \beta_3 + \ldots + \beta_N) + (\beta_1 + \beta_3 + \ldots + \beta_N) + \ldots (\beta_1 + \beta_2 + \ldots + \beta_{N-1}) \tag{47}$$

Calculating the common elements in equation (47), the second term can be redefined as a single summation.

$$\sum_{j=1}^{N}\left(\sum_{(i=1),(i\neq j)}^{N}\beta_i\right)=(N-1)\beta_1+(N-1)\beta_2+\ldots+(N-1)\beta_N=(N-1)\sum_{j=1}^{N}\beta_i \tag{48}$$

Substituting Equation (48) in Equation (46):

$$x\sum_{j=1}^{N}\beta_j+y(N-1)\sum_{j=1}^{N}\beta_j=\big(x+y(N-1)\big)\left(\sum_{j=1}^{N}\beta_j\right)=0 \tag{49}$$

As a result, we can draw the following conclusions:

First Conclusion $x=-y(N-1)$ (This is not true in our case)

Second Conclusion
$$\sum_{j=1}^{N}\beta_j=0 \tag{50}$$

Equation (50) allows us to create the following equation for any $j=1,2,\ldots,N$.

$$\beta_j=\sum_{(i=1),(i\neq j)}^{N}-\beta_i \tag{51}$$

Substituting Equation (51) into the general form of Equation (45):

Row # j
$$-x\sum_{(i=1),(i\neq j)}^{N}\beta_i+y\sum_{(i=1),(i\neq j)}^{N}\beta_i=0 \tag{52}$$

The following conclusions are obtained by factoring the common element in Equation (52):

First Conclusion $x=y$ (This is not true in our case)

Second Conclusion
$$\sum_{(i=1),(i\neq j)}^{N}-\beta_i=0=\beta_j \tag{53}$$

This indicates that $\boldsymbol{A}^{(1)}$ has a full rank property and that $\boldsymbol{\beta}=\boldsymbol{0}$ are vectors. Matrixes of the type in Equation (41) must meet the following general characteristics to be full rank:

$$x\neq -y(N-1) \tag{54}$$

$$x\neq y \tag{55}$$

Because $\boldsymbol{A}^{(2)}$ has the same structure as $\boldsymbol{A}^{(1)}$ and meets the general criteria in Equations (54) and (55), it follows that $\boldsymbol{A}_{\boldsymbol{T}}^{(2)}$ is also a full rank matrix.

Appendix B

According to Appendix A, the matrix $\boldsymbol{A}^{(3)}$ has a full rank property if and only if $\boldsymbol{A}_{\boldsymbol{T}}^{(3)}$ is a full rank. This means that if and only if $\boldsymbol{\beta} \in \mathbb{R}^N$, $\boldsymbol{\beta} = [\beta_1, \beta_2, \dots, \beta_N]^T$, and $\boldsymbol{A}_{\boldsymbol{T}}^{(3)}\boldsymbol{\beta} = \boldsymbol{0}$, the vector $\boldsymbol{\beta}$ must be equal to $\boldsymbol{0}$, that means $\beta_i = 0$ for $i = 1,2, \dots, N$, where $\beta_i \in \boldsymbol{\beta}$.

Defining a set of indexes $\boldsymbol{z}^{(k)} = \left\{z_1^{(k)}, z_2^{(k)}, z_3^{(k)}, z_4^{(k)}\right\}$, $k = \left(\left((row\ index) - 1\right) mod \frac{N}{4}\right) + 1$, mod is a modulo operation that represents the row index. In Equation (34) we define the index $z_i^{(k)}$ at $w = N/4$ as follows:

$$z_i^{(k)} = \frac{(i-1)N}{4} + k \tag{56}$$

To simplify the rest of the proof, we also define the following equation:

$$x\left(z_i^{(1)}\right) = 2\rho e^{\left(-2\rho\frac{z_i^{(1)}-1}{N}\right)} = \bar{x}_i \tag{57}$$

Recalling Equation (34), the vector $\boldsymbol{r}_{\boldsymbol{N/4}}$ has the following structure:

$$\boldsymbol{r}_{\boldsymbol{N/4}} = [\bar{x}_1, y, \dots, \bar{x}_2, y, \dots, \bar{x}_3, y, \dots, \bar{x}_4, y, \dots y] \tag{58}$$

The matrix $\boldsymbol{A}_{\boldsymbol{T}}^{(3)}$ corresponds to vector $\boldsymbol{r}_{\boldsymbol{N/4}}$. Equation (35) can be read as:

$$\boldsymbol{A}_{\boldsymbol{T}}^{(3)} = \begin{bmatrix} \bar{x}_1 & y & \cdots & \bar{x}_2 & y & \cdots & \bar{x}_3 & y & \cdots & \bar{x}_4 & y & \cdots \\ y & \ddots & \ddots & y & \ddots & \ddots & y & \ddots & \ddots & y & \ddots & \ddots \\ \vdots & \ddots & \bar{x}_1 & \ddots & \ddots & \bar{x}_2 & \ddots & \ddots & \bar{x}_3 & \ddots & \ddots & \bar{x}_4 \\ \bar{x}_4 & y & \ddots & \bar{x}_1 & y & \ddots & \bar{x}_2 & y & \ddots & \bar{x}_3 & y & \ddots \\ y & \ddots & \ddots & y & \ddots & \ddots & y & \ddots & \ddots & y & \ddots & \ddots \\ \vdots & \ddots & \bar{x}_4 & \ddots & \ddots & \bar{x}_1 & \ddots & \ddots & \bar{x}_2 & \ddots & \ddots & \bar{x}_3 \\ \bar{x}_3 & y & \ddots & \bar{x}_4 & y & \ddots & \bar{x}_1 & y & \ddots & \bar{x}_2 & y & \ddots \\ y & \ddots & \ddots & y & \ddots & \ddots & \ddots & \ddots & \ddots & y & \ddots & \ddots \\ \vdots & \ddots & \bar{x}_3 & \ddots & \ddots & \bar{x}_4 & \ddots & \ddots & \bar{x}_1 & \ddots & \ddots & \bar{x}_2 \\ \bar{x}_2 & y & \ddots & \bar{x}_3 & y & \ddots & \bar{x}_4 & \ddots & \ddots & \bar{x}_1 & y & \ddots \\ y & \ddots & \ddots & \ddots & \ddots & \ddots & \ddots & \ddots & \ddots & \ddots & \ddots & \ddots \\ \vdots & \cdots & \bar{x}_2 & y & \cdots & \bar{x}_3 & \cdots & \cdots & \bar{x}_4 & \cdots & \cdots & \bar{x}_1 \end{bmatrix} \tag{59}$$

Using Equation (59) and $\boldsymbol{A}_{\boldsymbol{T}}^{(3)}\boldsymbol{\beta} = \boldsymbol{0}$, we may create $N/4$ equation groups as shown below:

G #1

$$\beta_{z_1^{(k)}}\bar{x}_1 + \beta_{z_2^{(k)}}\bar{x}_2 + \beta_{z_3^{(k)}}\bar{x}_3 + \beta_{z_4^{(k)}}\bar{x}_4 + \sum_{(i=1),(i \notin z^{(k)})}^{N} \beta_i y = 0 \tag{60}$$

G #2

$$\beta_{z_1^{(k)}}\bar{x}_4 + \beta_{z_2^{(k)}}\bar{x}_1 + \beta_{z_3^{(k)}}\bar{x}_2 + \beta_{z_4^{(k)}}\bar{x}_3 + \sum_{(i=1),(i \notin z^{(k)})}^{N} \beta_i y = 0 \tag{61}$$

G #3
$$\beta_{z_1^{(k)}}\bar{x}_3 + \beta_{z_2^{(k)}}\bar{x}_4 + \beta_{z_3^{(k)}}\bar{x}_1 + \beta_{z_4^{(k)}}\bar{x}_2 + \sum_{(i=1),(i\notin z^{(k)})}^{N} \beta_i y = 0 \tag{62}$$

G #4
$$\beta_{z_1^{(k)}}\bar{x}_2 + \beta_{z_2^{(k)}}\bar{x}_3 + \beta_{z_3^{(k)}}\bar{x}_4 + \beta_{z_4^{(k)}}\bar{x}_1 + \sum_{(i=1),(i\notin z^{(k)})}^{N} \beta_i y = 0 \tag{63}$$

We obtain the following equations by adding up each group:

G #1
$$\sum_{k=1}^{\frac{N}{4}} \left(\beta_{z_1^{(k)}}\bar{x}_1 + \beta_{z_2^{(k)}}\bar{x}_2 + \beta_{z_3^{(k)}}\bar{x}_3 + \beta_{z_4^{(k)}}\bar{x}_4\right) + \sum_{k=1}^{\frac{N}{4}} \left(\sum_{(i=1),(i\notin z^{(k)})}^{N} \beta_i y\right) = 0 \tag{64}$$

G #2
$$\sum_{k=1}^{\frac{N}{4}} \left(\beta_{z_1^{(k)}}\bar{x}_4 + \beta_{z_2^{(k)}}\bar{x}_1 + \beta_{z_3^{(k)}}\bar{x}_2 + \beta_{z_4^{(k)}}\bar{x}_3\right) + \sum_{k=1}^{\frac{N}{4}} \left(\sum_{(i=1),(i\notin z^{(k)})}^{N} \beta_i y\right) = 0 \tag{65}$$

G #3
$$\sum_{k=1}^{\frac{N}{4}} \left(\beta_{z_1^{(k)}}\bar{x}_3 + \beta_{z_2^{(k)}}\bar{x}_4 + \beta_{z_3^{(k)}}\bar{x}_1 + \beta_{z_4^{(k)}}\bar{x}_2\right) + \sum_{k=1}^{\frac{N}{4}} \left(\sum_{(i=1),(i\notin z^{(k)})}^{N} \beta_i y\right) = 0 \tag{66}$$

G #4
$$\sum_{k=1}^{\frac{N}{4}} \left(\beta_{z_1^{(k)}}\bar{x}_2 + \beta_{z_2^{(k)}}\bar{x}_3 + \beta_{z_3^{(k)}}\bar{x}_4 + \beta_{z_4^{(k)}}\bar{x}_1\right) + \sum_{k=1}^{\frac{N}{4}} \left(\sum_{(i=1),(i\notin z^{(k)})}^{N} \beta_i y\right) = 0 \tag{67}$$

Equations ((64), (65), (66), and (67)) are added together to obtain:

$$\left(\sum_{j=1}^{4} \bar{x}_j\right) \sum_{k=1}^{\frac{N}{4}} \left(\beta_{z_1^{(k)}} + \beta_{z_2^{(k)}} + \beta_{z_3^{(k)}} + \beta_{z_4^{(k)}}\right) + \sum_{k=1}^{\frac{N}{4}} \sum_{j=1}^{4} \left(\sum_{(i=1),(i\notin z^{(k)})}^{N} \beta_i y\right) = 0 \tag{68}$$

We observe that the total of all elements β equals the initial summation. Simplifying Equation (68) by doing the following:

$$\sum_{k=1}^{\frac{N}{4}} \sum_{j=1}^{4} \left(\sum_{(i=1),(i\notin z^{(k)})}^{N} \beta_i y\right) = 4y \sum_{k=1}^{\frac{N}{4}} \left(\sum_{(i=1),(i\notin z^{(k)})}^{N} \beta_i\right) = 4y\left(\frac{N}{4} - 1\right) \sum_{i=1}^{N} \beta_i \tag{69}$$

Then Equation (68) can be rewritten as:

$$\left(\sum_{j=1}^{4} \bar{x}_j\right)\left(\sum_{i=1}^{N} \beta_i\right) + 4y\left(\frac{N}{4} - 1\right) \sum_{i=1}^{N} \beta_i \tag{70}$$

Either $\qquad \left(\sum_{j=1}^{4} \bar{x}_j\right) = -4y\left(\frac{N}{4} - 1\right)$ which is not true.

Or

$$\sum_{i=1}^{N} \beta_i = 0 \tag{71}$$

For any value of k and from Equation (71) we have:

$$\sum_{(i=1),(i\notin z^{(k)})}^{N} \beta_i = \sum_{(i=1),(i\in z^{(k)})}^{N} -\beta_i \tag{72}$$

We obtain the following new set of equations by substituting Equation (72) in Equations ((60), (61), (62) and (63)):

G #1 $$\beta_{z_1^{(k)}}(\bar{x}_1 - y) + \beta_{z_2^{(k)}}(\bar{x}_2 - y) + \beta_{z_3^{(k)}}(\bar{x}_3 - y) + \beta_{z_4^{(k)}}(\bar{x}_4 - y) = 0 \tag{73}$$

G #2 $$\beta_{z_1^{(k)}}(\bar{x}_4 - y) + \beta_{z_2^{(k)}}(\bar{x}_1 - y) + \beta_{z_3^{(k)}}(\bar{x}_2 - y) + \beta_{z_4^{(k)}}(\bar{x}_3 - y) = 0 \tag{74}$$

G #3 $$\beta_{z_1^{(k)}}(\bar{x}_3 - y) + \beta_{z_2^{(k)}}(\bar{x}_4 - y) + \beta_{z_3^{(k)}}(\bar{x}_1 - y) + \beta_{z_4^{(k)}}(\bar{x}_2 - y) = 0 \tag{75}$$

G #4 $$\beta_{z_1^{(k)}}(\bar{x}_2 - y) + \beta_{z_2^{(k)}}(\bar{x}_3 - y) + \beta_{z_3^{(k)}}(\bar{x}_4 - y) + \beta_{z_4^{(k)}}(\bar{x}_1 - y) = 0 \tag{76}$$

At any value of k, the last four equations can be represented as a vector-matrix multiplication:

$$\begin{bmatrix} (\bar{x}_1 - y) & (\bar{x}_2 - y) & (\bar{x}_3 - y) & (\bar{x}_4 - y) \\ (\bar{x}_4 - y) & (\bar{x}_1 - y) & (\bar{x}_2 - y) & (\bar{x}_3 - y) \\ (\bar{x}_3 - y) & (\bar{x}_4 - y) & (\bar{x}_1 - y) & (\bar{x}_2 - y) \\ (\bar{x}_2 - y) & (\bar{x}_3 - y) & (\bar{x}_4 - y) & (\bar{x}_1 - y) \end{bmatrix} \begin{bmatrix} \beta_{z_1^{(k)}} \\ \beta_{z_2^{(k)}} \\ \beta_{z_3^{(k)}} \\ \beta_{z_4^{(k)}} \end{bmatrix} = \begin{bmatrix} 0 \\ 0 \\ 0 \\ 0 \end{bmatrix} \tag{77}$$

Since the determinant of the 4×4 matrix in Equation (77) is not zero due to its full rank property, the vector $\left[\beta_{z_1^{(k)}} \quad \beta_{z_2^{(k)}} \quad \beta_{z_3^{(k)}} \quad \beta_{z_4^{(k)}}\right]^T$, has to be the null vector. Since $k = 1,2,\ldots,\frac{N}{4}$, all of the elements of vector β must be zero, leading to $\boldsymbol{A}^{(3)}$ being a full rank matrix in this case. The following general conditions must be met for $\boldsymbol{A}^{(3)}$ to full rank matrix:

$$\left(\sum_{j=1}^{4} \bar{x}_j\right) \neq -4y\left(\frac{N}{4} - 1\right) \tag{78}$$

$$\begin{bmatrix} (\bar{x}_1 - y) & (\bar{x}_2 - y) & (\bar{x}_3 - y) & (\bar{x}_4 - y) \\ (\bar{x}_4 - y) & (\bar{x}_1 - y) & (\bar{x}_2 - y) & (\bar{x}_3 - y) \\ (\bar{x}_3 - y) & (\bar{x}_4 - y) & (\bar{x}_1 - y) & (\bar{x}_2 - y) \\ (\bar{x}_2 - y) & (\bar{x}_3 - y) & (\bar{x}_4 - y) & (\bar{x}_1 - y) \end{bmatrix} \tag{79}$$

must be full rank

References

[1] Al-Jzari, A., & Iviva, K. (2015). Cyclic Prefix Length Determination for Orthogonal Frequency Division Multiplexing System over Different Wireless Channel Models Based on the Maximum Excess Delay Spread. *American Journal of Engineering and Applied Sciences*, *8*(1), 82–93.

[2] Al-Qadhi, O., Abdul-Rahaim, L., Sahib, D., Obaid, A., & Alwan, F. (2024). Subspace Blind Channel Estimation Methods in OFDM Systems under Multi-path Channels. *Research Article*. https://doi.org/10.21203/rs.3.rs-3792522/v1

[3] Al-Qadhi, O., Semenov, E., Talib, J., Al-Barrak, S., & Al-Ghazali, M. (2024). Blind channel estimation in ZP-OFDM system using new precoding matrix over channels with memory. *In E3S Web of Conferences*, EDP Sciences, *474*, 02025. https://doi.org/10.1051/e3sconf/202447402025

[4] Al-Qadhi, O., Semenov, E., Talib, J., Almufti, A., & Al-Ghazali, M. (2023). New precoding blind channel estimation and channel order estimation algorithm in OFDM systems with cyclic prefix. *(D. Nazarov & A. Juraeva, Eds.) E3S Web of Conferences*, *419*, 02022. https://doi.org/10.1051/e3sconf/202341902022

[5] Andersen, J.B., Rappaport, T.S., & Yoshida, S. (1995). Propagation measurements and models for wireless communications channels. *IEEE Communications magazine*, *33*(1), 42-49.

[6] Coleri, S., Ergen, M., Puri, A., & Bahai, A. (2002). Channel estimation techniques based on pilot arrangement in OFDM systems. *IEEE Transactions on broadcasting*, *48*(3), 223-229.

[7] Dou, C., & Wang, L.S. (2010). Fading effects on the lower shifting of mode switching thresholds in the rate adaptive IEEE 802.11 a/g WLANs. *International Journal of Communications, Network and System Sciences*, *3*(8), 655.–667.

[8] Doukopoulos, X.G., & Moustakides, G.V. (2004). Adaptive algorithms for blind channel estimation in OFDM systems. *In IEEE International Conference on Communications*, *4*, 2377-2381.

[9] Doukopoulos, X.G., & Moustakides, G.V. (2006). Blind adaptive channel estimation in OFDM systems. *IEEE Transactions on Wireless Communications*, *5*(7), 1716-1725.

[10] Fan, W., Gao, F., & Xue, Y. (2009). A New Blind Channel Estimation Algorithm for OFDM Systems. *In 2nd International Congress on Image and Signal Processing*, 1-4.

[11] Fang, S.H., Chen, J.Y., Lin, J.S., Shieh, M.D., & Hsu, J.Y. (2015). Blind channel estimation for CP/CP-free OFDM systems using subspace approach. *In IEEE 81st Vehicular Technology Conference (VTC Spring)*, 1-5.

[12] Gao, F., & Nallanathan, A. (2007). Blind channel estimation for OFDM systems via a generalized precoding. *IEEE Transactions on Vehicular Technology*, *56*(3), 1155-1164.

[13] Heinz, C., Zuppelli, M., & Caviglione, L. (2021). Covert Channels in Transport Layer Security: Performance and Security Assessment. *Journal of Wireless Mobile Networks, Ubiquitous Computing, and Dependable Applications (JoWUA)*, *12*(4), 22-36.

[14] Li, Y., Cimini, L.J., & Sollenberger, N.R. (1998). Robust channel estimation for OFDM systems with rapid dispersive fading channels. *IEEE Transactions on Communications*, *46*(7), 902–915.

[15] Liang, Y., Luo, H., Xu, Y., & Huang, J. (2006). Blind Channel Estimation Based on Linear Precoding for OFDM Systems. *International Conference on Wireless Communications, Networking and Mobile Computing*, 1–4.

[16] Lin, R., & Petropulu, A.P. (2003). Linear block precoding for blind channel estimation in OFDM systems. *In Seventh International Symposium on Signal Processing and Its Applications*, *2*, 395-398.

[17] Lin, R., & Petropulu, A.P. (2005). Linear precoding assisted blind channel estimation for OFDM systems. *IEEE Transactions on Vehicular Technology*, *54*(3), 983-995.

[18] Mostofi, Y., & Cox, D.C. (2005). ICI mitigation for pilot-aided OFDM mobile systems. *IEEE Transactions on Wireless Communications*, *4*(2), 765–774.

[19] Muquet, B., De Courville, M., & Duhamel, P. (2002). Subspace-based blind and semi-blind channel estimation for OFDM systems. *IEEE Transactions on signal processing*, *50*(7), 1699-1712.

[20] Petropulu, A., & Zhang, R. (2002). Blind channel estimation for OFDM systems. In *10th IEEE Digital Signal Processing Workshop, DSP 2002 and the 2nd IEEE Workshop on Signal Processing Education, SPE 2002*. Institute of Electrical and Electronics Engineers Inc, 366-370.

[21] Petropulu, A., Zhang, R., & Lin, R. (2004). Blind OFDM channel estimation through simple linear precoding. *IEEE Transactions on Wireless Communications*, *3*(2), 647-655.

[22] Sari, H., Karam, G., & Jeanclaude, I. (1995). Transmission techniques for digital terrestrial TV broadcasting. *IEEE Communications Magazine*, *33*(2), 100–109.

[23] Schott, J. R. (2017). Matrix analysis for statistics. Hoboken, New Jersey: Wiley.

[24] Xuejun, H., Houjie, B., & Songyu, Y. (2003). A new subspace algorithm of blind channel estimation for OFDM systems. *In 14th IEEE Proceedings on Personal, Indoor and Mobile Radio Communications, 2*, 1105-1108.

[25] Yongming, L., Hanwen, L., Yadong, W., & Jianguo, H. (2007). Blind channel estimation for redundant precoded OFDM systems. *Journal of Systems Engineering and Electronics*, *18*(4), 692-697.

[26] Yue, X., & Zhou, X. (2011). Blind channel estimation for CP-free OFDM communications systems. *In Eighth International Conference on Fuzzy Systems and Knowledge Discovery (FSKD), 4*, 2254-2257.

[27] Zeng, Y., & Ng, T.S. (2004). A proof of the identifiability of a subspace-based blind channel estimation for OFDM systems. *IEEE Signal Processing Letters*, *11*(9), 756-759.

[28] Zhang, R. (2005). Blind channel estimation for precoded OFDM system. *In Proceedings. (ICASSP'05). IEEE International Conference on Acoustics, Speech, and Signal Processing, 3*, 3-469.

[29] Zhou, S., Muquet, B., & Giannakis, G.B. (2002). Subspace-based (semi-) blind channel estimation for block precoded space-time OFDM. *IEEE Transactions on Signal Processing*, *50*(5), 1215-1228.

Authors Biography

Osamah J. Al-Qadhi was born in Al-Hilla city, Iraq. He received bachelor degree in general electrical engineering from the University of Babylon in Iraq, master degree in information technologies and communication systems from Kazan National Research Technical University in Russia, and PhD degree from Volgograd State University in the specialty of electronics, radio, and communication systems. His research interests include digital and wireless communications systems, signal processing with OFDM and MIMO systems, channel estimation in OFDM systems, algorithms, data structures and graph theory.

Laith A. Abdul-Rahaim is currently the dean of the college of engineering at Babylon University and also a lecturer at the Department of Electrical Engineering at the University of Babylon. He received Ph.D. degree in electrical engineering from the University of Technology in Iraq. He researches in digital communication systems design, information science, Radio Propagation, Microwave Communication, Data Compression, Digital Speech Processing, Wireless Ad Hoc Networks, OFDM systems and Cellular Networks. He has a professor degree in wireless communication.